NASA/TM—2001-210602

Longtime Durability of PMR–15 Matrix Polymer at 204, 260, 288, and 316 °C

Kenneth J. Bowles
Glenn Research Center, Cleveland, Ohio

Demetrios S. Papadopoulos
University of Akron, Akron, Ohio

Linda L. Inghram and Linda S. McCorkle
Ohio Aerospace Institute, Brook Park, Ohio

Ojars V. Klan
Glenn Research Center, Cleveland, Ohio

National Aeronautics and
Space Administration

Glenn Research Center

July 2001

Available from

NASA Center for Aerospace Information
7121 Standard Drive
Hanover, MD 21076

National Technical Information Service
5285 Port Royal Road
Springfield, VA 22100

Available electronically at http://gltrs.grc.nasa.gov/GLTRS

LONGTIME DURABILITY OF PMR–15 MATRIX POLYMER AT 204, 260, 288, AND 316 °C

Kenneth J. Bowles
National Aeronautics and Space Administration
Glenn Research Center
Cleveland, Ohio 44135

Demetrios S. Papadopoulos
University of Akron
Akron, Ohio 44325

Linda L. Inghram and Linda S. McCorkle
Ohio Aerospace Institute
Brook Park, Ohio 44142

Ojars V. Klan
National Aeronautics and Space Administration
Glenn Research Center
Cleveland, Ohio 44135

SUMMARY

Isothermal weight loss studies at the Glenn (Lewis) Research Center were conducted at four temperatures (204, 260, 288, and 316 °C) with specimens of varied geometric shapes to investigate the mechanisms involved in the thermal degradation of PMR–15. Both neat resin behavior and composite behaviors were studied. Two points of interest in these studies are the role(s) of oxygen in the mechanisms involved in the thermo-oxidative degradation of these composite materials and the dimensional changes that occur during their useable lifetime.

Specimen dimensional changes and surface layer growth were measured and recorded. It was shown that physical and chemical changes take place as a function of time and location in PMR–15 neat resin and composites as aging takes place in air at elevated temperatures. These changes initiate at the outer surfaces of both materials and progress inward following the oxygen as it proceeds by diffusion into the central core of each material. Microstructural changes cause changes in density, material shrinkage (strains), glass transition temperature, dimension, dynamic shear modulus, and compression properties. These changes also occur slowly, dividing the polymer material into two distinct parts: a visibly undamaged core section between two visibly damaged surface layers. The surface layer has a significant effect on compression properties of thinner specimens, but the visibly undamaged core material controls these properties for specimens having eight or more plies. It was demonstrated that there are three different mechanisms involved in the degradation of PMR–15 during aging at elevated temperatures. These are a weight gain, a small weight fraction bulk material weight loss, and a large mass fraction weight loss concentrated at the surface of the polymer or composite. At the higher temperatures (260 °C and above), the surface loss predominates. Below 260 °C, the surface loss and the bulk core loss become more equivalent. Between 175 and 260 °C, the initial weight change is due to a weight gain mechanism with a visible lifetime that diminishes as the aging temperature increases.

INTRODUCTION

Recent publications have addressed the need for the development of a reliable, predictive mechanistic model to describe the effects of elevated-temperature isothermal aging of polymer matrix composites on the mechanical and chemical durability of these materials (refs. 1 to 4). A coupled reaction-diffusion model was used to identify the degradation mechanism. The mechanisms that are considered for modeling are based on either diffusion-controlled degradation or reaction-controlled oxygen effects (refs. 1 to 5). These studies considered two extreme conditions that

were based on oxygen consumption rates. At one extreme, the consumption rate in the polymer was low, and the reaction rate of the oxygen with the core of the material was controlling. At the other extreme, the reactions in the composite and neat resin readily digested the oxygen as it diffused into the surface material, the reaction being controlled by the availability of oxygen. Thus, diffusion controlled the degradation process. Both neat resin behavior and composite behaviors were studied. Two points of interest in these studies are the roles that oxygen played in the mechanisms involved in the thermo-oxidative degradation of these composite materials and the dimensional changes that occurred during their useable lifetime.

Isothermal weight loss studies at the Glenn Research Center were conducted at four temperatures with specimens of varied geometric shapes to further investigate the mechanisms involved in the thermal degradation of PMR–15. The dimensional changes and surface layer growth were measured and recorded. The data were in agreement with those published in references 1 and 2. An initial weight increase reaction was observed to be dominating at the lower temperatures. However, at the more elevated temperatures, the weight loss reactions were prevalent and masked the weight gain reaction. These data confirmed the findings of the existence of a weight gain reaction published in reference 2. Surface-dependant weight loss was shown to control the polymer degradation at the higher temperatures.

MATERIALS STUDIED

Some of the materials data presented herein were obtained from references 1 to 6. The materials used in references 1, 3, and 4 to 6 were processed at the Glenn Research Center. The details of the processing for these materials are also available in these publications. The new data reported herein were measured at the Glenn Research Center. Materials were fabricated in matched metal die molds in the form of neat resin PMR–15 and were cured at 316 °C for 2 hr. All materials except those processed in reference 6 were postcured in air at 316 °C for 16 hr. The quality of these materials was confirmed by nondestructive evaluation procedures and by metallographic photography during aging.

Specimens of different sizes were machined to size by a water-cooled micromachining diamond saw. The dimensions, surface areas, and volumes of the specimens are listed in table I.

TABLE I.—DIMENSIONS, VOLUMES, AND SURFACE AREAS OF NEAT RESIN SPECIMENS

Temperature, °C	Length, L, cm	Width, w, cm	Thickness, t, cm	Volume, V, cm^3	Surface area, S, cm^2
316	3.90	0.73	0.106	4.97	40.42
	3.90	.49	.102	3.29	28.46
	1.99	.50	.104	1.70	14.84
	1.99	.49	.105	1.71	14.92
288	4.00	0.99	0.109	7.16	57.51
	4.00	.49	.110	3.62	31.32
	1.99	1.02	.111	3.73	29.96
	2.01	.50	.111	1.85	16.43
	1.99	.49	.111	1.83	16.03
260	3.90	1.00	0.105	6.77	56.51
	3.90	.50	.101	3.26	30.61
	1.99	.99	.103	3.36	29.37
	1.99	.50	.105	1.73	17.56
204	3.90	0.99	0.103	6.63	56.70
	3.90	.49	.099	3.16	30.45
	1.99	1.00	.101	3.35	21.51
	1.99	.49	.106	1.73	16.13

TESTING

The polymer specimens were aged in air-circulating ovens after drying at 125 °C for 24 hr to remove all moisture. The oven airflow rates were maintained at 100 cm^3/min. The study temperatures of 204, 260, 288, and 316 °C were measured by nine calibrated thermocouples as specified in ANSI/ASTM E 145–68. The specimens were removed from the ovens at regular intervals and placed in a desiccator where they cooled to room temperature.

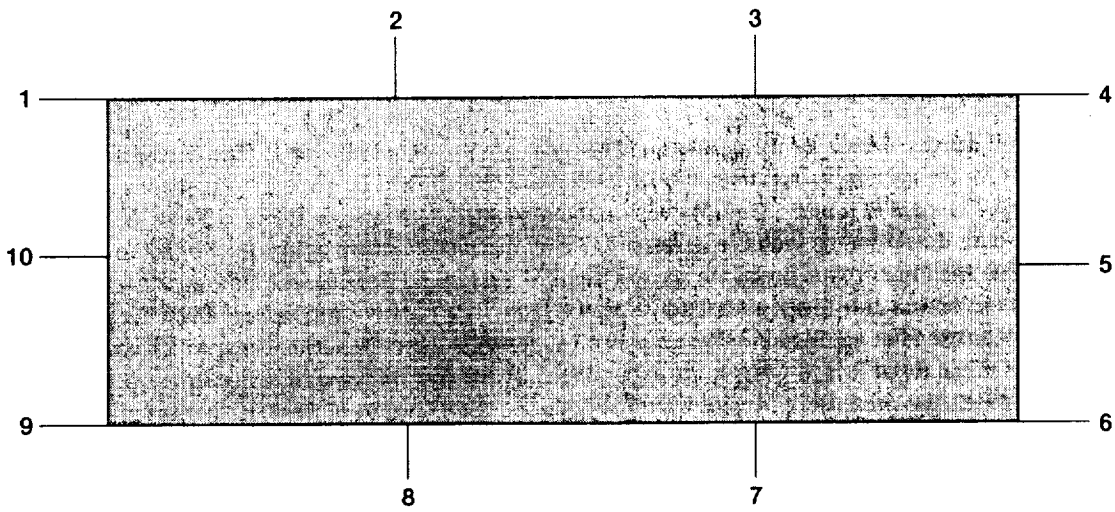

Figure 1.—Marked index position for dimensional measurements. Total measurements made: 10 thicknesses, 4 widths, 3 lengths (1–4; 4–6; 6–9; 9–1; 7–3; 8–2; 10–5).

The specimens were not removed from the desiccator until they were weighed. After the weights were recorded, the dimensions were measured and metallographic samples were removed for examination of the surface layers. They were then returned to the ovens. The maximum aging time was limited to approximately 4000 hr.

Dimensional measurements were made using a Nicon Measurescope 10 traveling microscope with an accuracy of ±0.00127 mm. Ten separate measurements were made of each specimen thickness at indexed points around the perimeter as shown in figure 1. Seven length and width measurements were made at the same indexed locations; that is, a total of three length and four width measurements was recorded. Average values of the dimensions were used in all calculations. In some instances there were uncertainties in the length measurements because the polymer specimens were warped.

Glass transition temperatures T_G for the neat polymer and composites were measured by dynamic mechanical analysis (DMA) testing. A Rheometrics RMS–800 rheological spectrometer was used to take measurements of the rectangular test pieces. The two components of the complex shear modulus were measured as a function of temperature. The test pieces were stressed in torsion across the specimen widths. The heating rate was 5 °C/min, the frequency was 6.28 radians/s, and the strain was 0.2. All specimens were dried in an air-circulating oven at 125 °C for 24 hr before they were tested. This was a sufficient amount of time to reduce the moisture content to very low levels. The glass transition temperature was determined by measuring the intersection of the two tangents to the linear portions of the stored shear modulus G' curve where it suddenly dropped to a minimum.

The densities of neat resin were measured as specified in ASTM D–792 before aging and after approximately 4000 hr of aging at the four elevated temperatures.

All compression tests of the composite specimens were performed according to the conditions specified in "Test Method for Compressive Properties of Rigid Plastics" (ASTM D–695M): crosshead speed, 1.2 mm/min; temperature, 23.3 °C; and relative humidity, 50 percent. The specimens were conditioned at 125 °C for 16 hr before compression tests were conducted. No end tabs were used. Strain was measured with an extensometer, and moduli were measured using strains and loads at 500 and 1500 microstrain.

A traveler specimen was aged with the polymer test specimens. Small slices were removed from the traveler when the test specimens were removed for weighing and dimensional measurements. The layer thickness measurements were made from photomicrographs taken using differential interference contrast to accentuate the changes in gray tones at the damage surface interface with the visibly undamaged core. The final polishing medium used to prepare the mounted specimen was a 0.05-micron colloidal silica emulsion.

The fiber contents of the composites were measured by acid digestion as described in ASTM D–3171. The void content was calculated as the difference between the specific volume of a composite specimen (measured using the immersion technique as specified in ASTM D–792) and the theoretical specific volume calculated from the acid digestion results. The differences were divided by the measured specific volume and multiplied by 100 to give the void volume in percent. The densities of the resin and fiber were taken to be 1.32 and 1.78 g/cm^3, respectively.

RESULTS

Density Changes

The measured density values for the neat resin specimens are presented in table II. The densities increased by about 1.5 percent for the specimens aged for 4000 hr at 204 and 260 °C and by almost 0.9 percent after aging for 3300 hr at 316 °C. The data in figure 2 (ref. 5) confirm the measured data in table II and indicate that neat resin specimens aged in air do exhibit an increase in density during thermo-oxidative aging. In contrast to this observation, the specimens aged in nitrogen appear to show a trend of decreasing density with time at temperature. These data suggest that the central core is not completely isolated from the oxidative atmosphere since the measured density is shown to increase after aging in air. The data also suggest that thermal mechanisms, which cause a decrease in volume and an initial rapid loss in weight, are experienced by the specimens aged at higher temperatures (above 260 °C). In both cases, the decreasing density is probably due to the diffusion of gaseous cure reaction products from the bulk of the specimens.

The densities of the fabric-reinforced composites aged at elevated temperatures for extended time periods were calculated from before and after weight and dimension measurements made during aging from data presented in reference 1. The results are presented in table III. The composite specimens aged at the lower temperatures had measured densities greater than the initial values, thus indicating an increase in weight and/or a decrease in volume during the aging period.

Dynamic Mechanical Analysis

Figure 3 shows the data for the neat resin specimens aged at 316, 288, 260, and 204 °C for 2534, 4072, 4312, and 4200 hr, respectively. Unaged specimen data are also presented for reference. It is evident that significant crosslinking continues during the duration of aging for the specimens aged at 316 and 260 °C. This crosslinking probably contributes to the shrinkage in the volume of the polymer. The stored shear moduli for the specimens aged at 316 and 204 °C are lower than that for the specimen aged at 260 °C because the surfaces of the two specimens had experienced cracking during the aging period. Cracks on the surface of the specimens aged at 316 °C penetrated farther into the thickness than those on the surfaces of the specimens aged at 204 °C.

Some 6.35-mm-thick T650–35 fabric/PMR–15 composite test pieces were machined as shown in table IV (ref. 7). Figure 4 presents a plot of the measured stored shear modulus for four specimens from different positions through the thickness of a specimen aged for 2090 hr at 316 °C. The first cut is not shown in table III because most of the matrix material was oxidized away. The data in curve 1 (curve 2 in fig. 4) are for the machined specimen containing the partially oxidized surface layer. The numbering increases with the depth through the original specimen, with curve 4 being close to the center of the specimen. The surface test piece (not shown in table III) has a stored modulus about 2 orders of magnitude less than the central pieces. This value is attributed to the very low amount of matrix at the surface. The glass transition temperatures T_G of specimens 1 and 2, as measured by the interception of the two stored modulus slopes, are greater than those of specimens 3 and 4, which indicates that there is a gradient of degradation through the core of the aged composite. The glass transition temperatures and stored moduli of these specimens are also greater than those of the neat resin aged for 2534 hr at the same temperature. The greater modulus is due to the influence of the carbon fabric reinforcement.

Thermo-Oxidative Stability

The neat resin weight loss data measured in this study at the four temperatures are presented in figure 5. The data in this figure were measured from specimens that were nominally 5.08 by 12.7 by 2 mm to assure that no geometric effects would bias the comparison of data measured at different temperatures. The maximum data point for the material aged at 316 °C is limited to the weight loss at 2800 hr because surface cracks began to form and the weight loss accelerated. Weight loss data for specimens aged at temperatures above 288 °C indicate that the weight loss is a function of the surface area. This relationship is shown in figure 6 where the weight losses for specimens with different surface areas (see table I) are plotted against surface area and specimen volume. When the aging temperature is reduced to 204 °C, the weight loss data shown in figure 7 appear to be partially dependent on both the

TABLE II.—DENSITIES OF NEAT RESIN SPECIMENS

Material	Sample number	Aging temperature, °C	Aging time, hr	Density, ρ, g/cm³
PMR–15	1	204	4400	1.339
	2			1.335
	3			1.337
	4	260	4300	1.336
	5			1.334
	6			1.339
	7	316	2800	1.332
	8			1.327
	9			1.327
	11	Unaged	Unaged	1.317
	12			1.315
	13			1.320

TABLE III.— DENSITIES AND FIBER CONTENTS OF T650–35/PMR–15 COMPOSITE

[From ref. 7]

Sample number	Aging temperature, °C	Aging time, hr	Density, ρ, g/cm³	Fiber, wt %
1	316	500	1.530	64.11
2			1.535	64.80
3			1.506	64.22
4	316	500	1.535	68.51
5			1.556	66.96
6			1.558	67.98
7	Unaged	Unaged	1.584	67.89
8			1.578	67.09
9			1.571	67.99
10	Unaged	Unaged	1.588	68.84
11			1.595	68.28
12			1.588	69.22

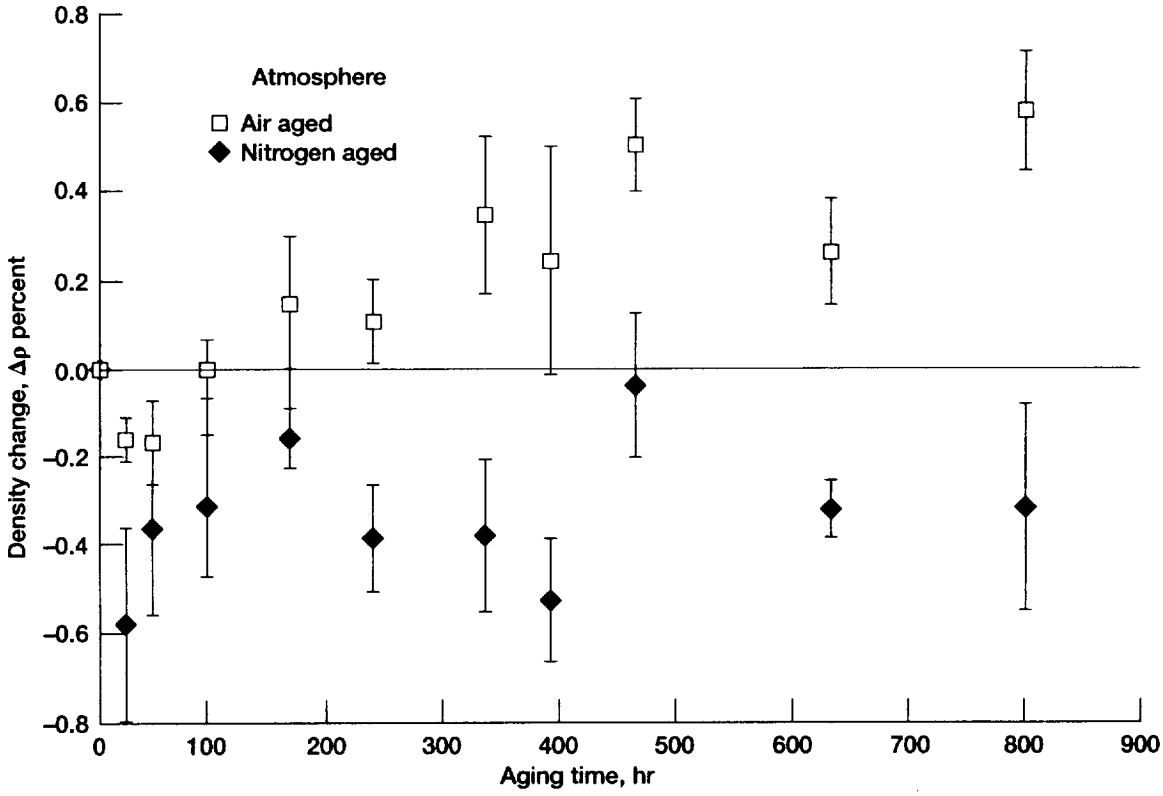

Figure 2.—Density changes of PMR–15 neat resin specimens during aging in air and nitrogen at 316 °C (ref. 5).

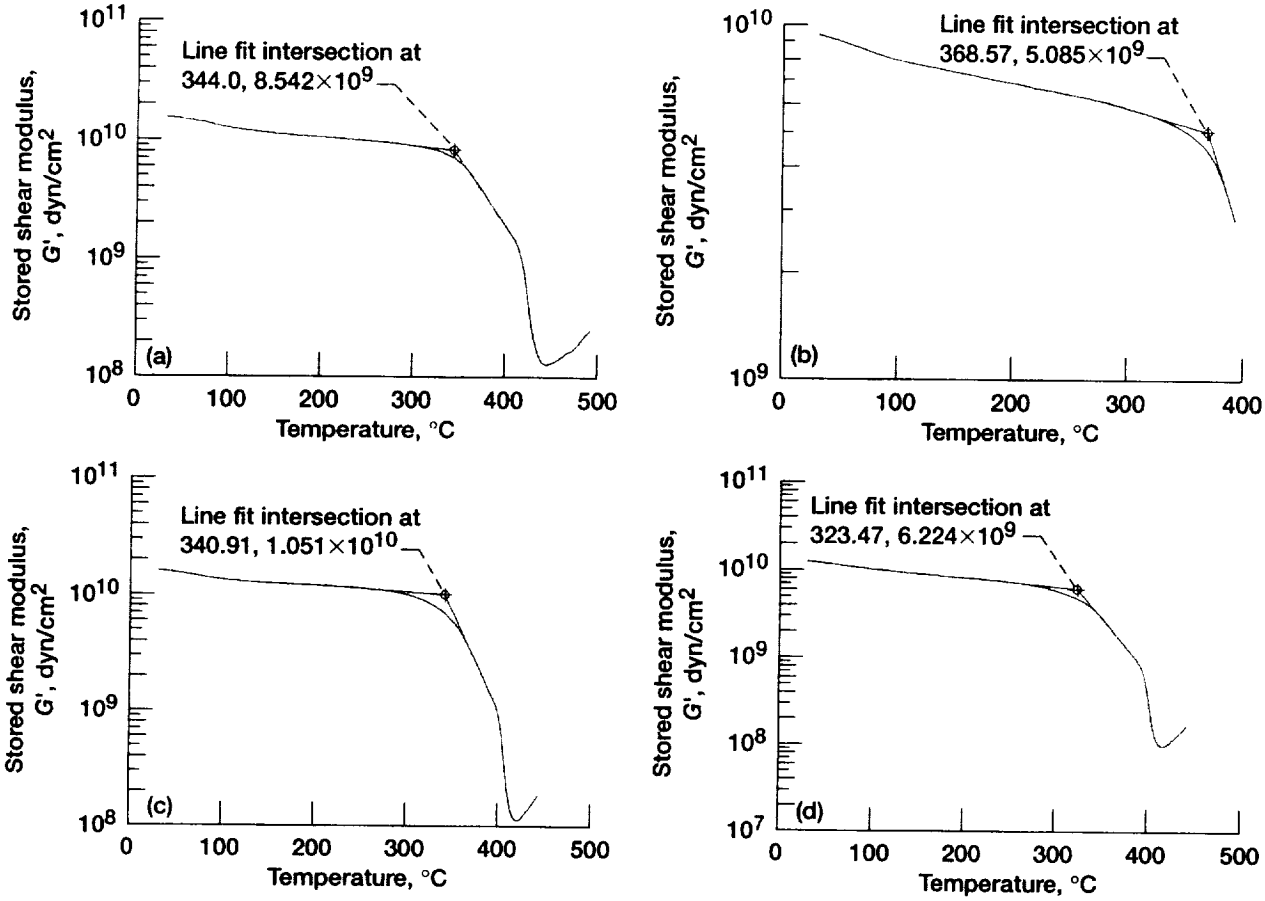

Figure 3.—Dynamic shear modulus measurements of PMR–15 neat resin specimens after aging. (a) No aging. (b) 316 °C for 2534 hr. (c) 260 °C for 4312 hr. (d) 204 °C for 4200 hr.

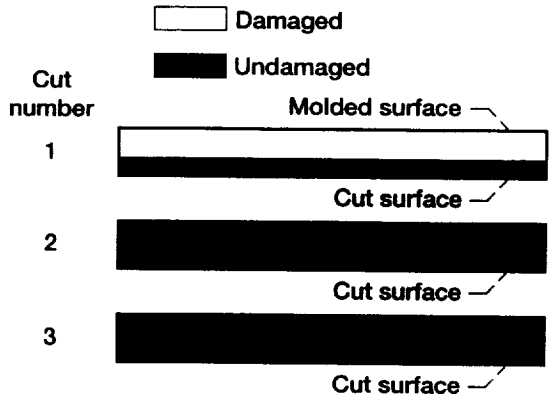

TABLE IV.—COMPRESSION STRENGTHS AND MODULI OF COMPOSITE SPECIMENS*

Cut number	Strength, MN/m^2	Modulus, GN/m^2
1	137.3	56.9
2	299.6	56.7
3	264.6	62.9

*Taken from different depths through the thickness of thick laminate aged at 260 °C for 20 000 hr.

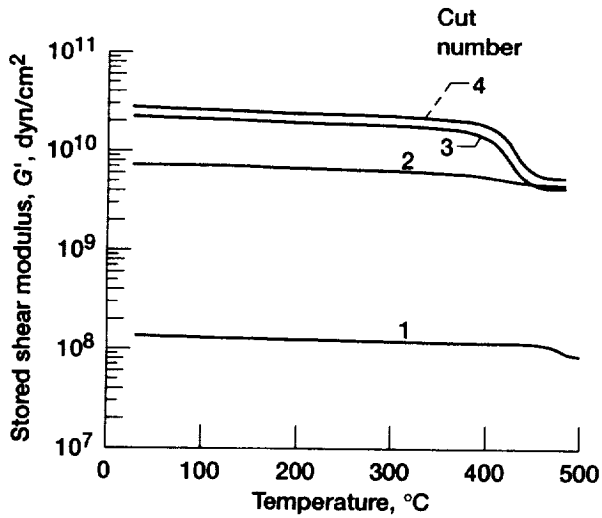

Figure 4.—Stored moduli of T650–35/PMR–15 composite specimens located at different distances from resin-rich surfaces in thickness direction of 20-ply plate. Plate aged in air at 360 °C for 2090 hr.

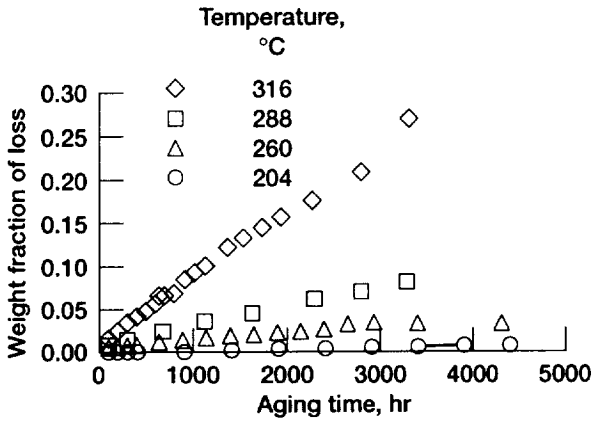

Figure 5.—Weight loss fraction of PMR–15 neat resin specimens as function of aging time and temperature.

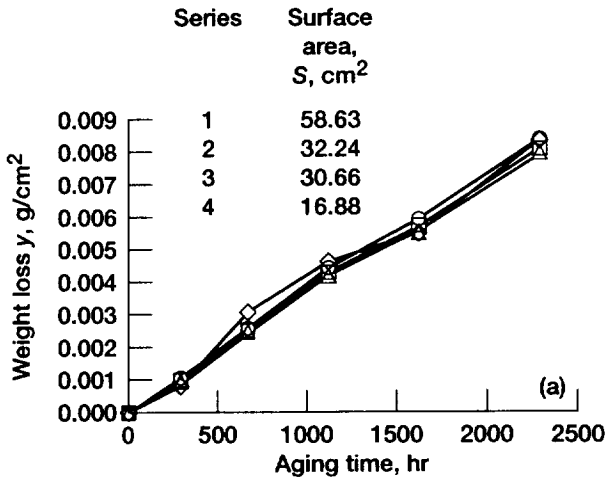

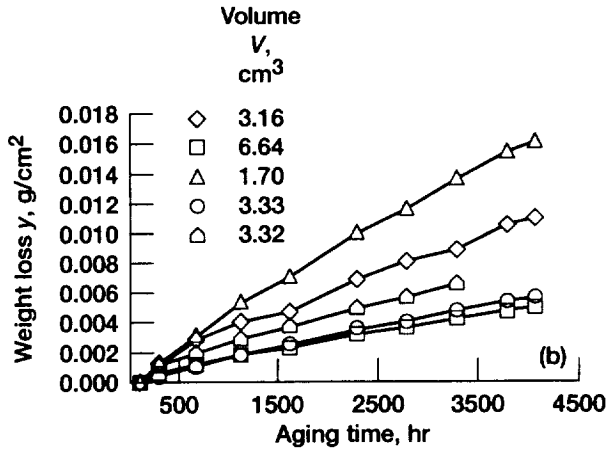

Figure 6.—Weight loss fraction of PMR–15 neat resin specimens as function of aging time and specimen surface area and volume. Polymer aged at 288 °C. (a) Surface area. (b) Volume.

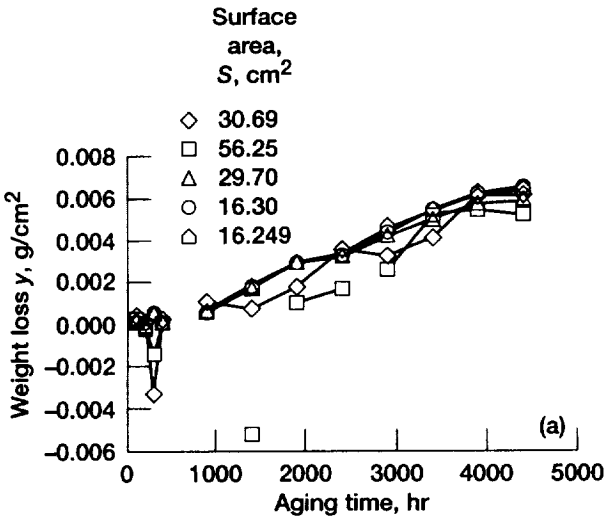

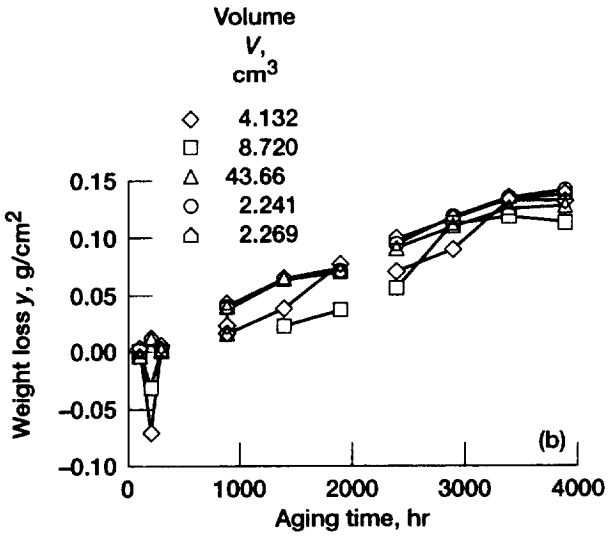

Figure 7.—Weight loss fraction of PMR–15 neat resin specimens as function of aging time and specimen surface area and volume. Polymer aged at 204 °C. (a) Surface area. (b) Volume.

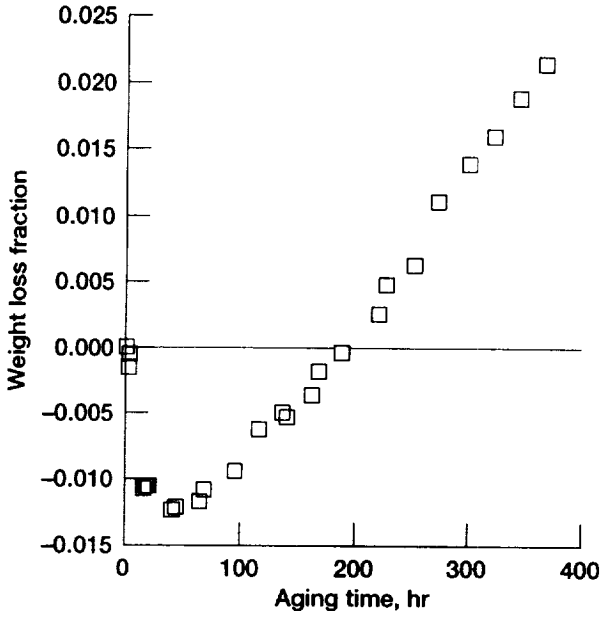

Figure 8.—Weight loss fraction of PMR–15 neat resin specimens as function of aging time at 225 °C. Weight gain mechanisms predominate during first 200 hr of aging (ref. 2).

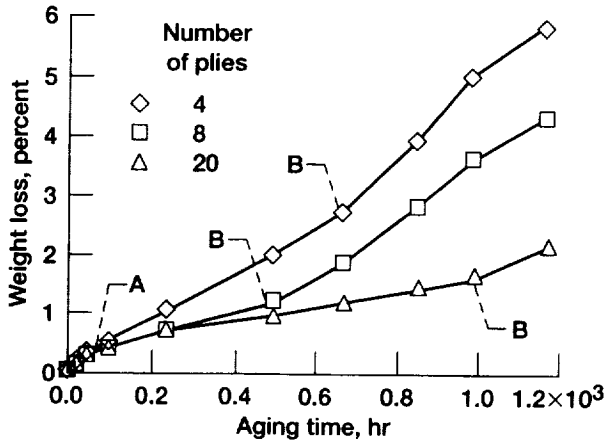

Figure 9.—Weight loss percent of T650–35/PMR–15 composites as function of aging time and specimen thickness at 316 °C.

surface area and the volume. The slight spread in data at longer times is due to the decrease in specimen dimensions over the duration of aging. This spread resulted in a decrease in surface areas and volumes. The initial (unaged) areas and volumes were used in all calculations. The slope of a straight line through the data gives a constant value of weight loss per unit volume per hour or a weight loss per unit area per hour. Thus, to accurately compare weight loss data on a percent basis, the specimen surface areas must be similar.

Ultrasonic C-scans indicate a degradation of the polymer during aging. This degradation is probably due to a mechanism that involves a loss of weight at a much lower rate than that from the surfaces because of the slow rate of diffusion of degradation products from the core material. Initially, as seen in figure 8 (ref. 2), a weight gain occurred in specimens aged at temperatures of 225 °C and below and was probably due to reactions such as carbonyl formation and thermo-oxidative crosslinking. The observed weight loss is consistent with the more intensive (shorter time between measurements) lower temperature thermo-oxidative study results reported in reference 2. No mass changes were observed at 150 °C, but changes were observed at 175 °C and above. The durations of time during which the weight gain persisted were 600 plus hr at 175 °C and 50 hr at 250 °C.

It is appropriate to compare the composite degradation mechanisms with those of the neat resin. Typical weight loss plots for T650–35 fabric/PMR–15 composites aged in air at 316 °C are shown in figure 9. The data can be divided into three different sections. From the origin to point A, there is a rapid increase in weight loss proportional to the volume of the specimen. Again, this increase is attributed to the diffusion of gaseous cure and postcure reaction products from the samples. Carbon dioxide (CO_2), carbon monoxide (CO), and water (H_2O) make up the dominant group of degradation products released during elevated temperature exposure (ref. 2). At temperatures below 350 °C, CO_2 is the predominant reaction product (ref. 2). Carbon monoxide begins to evolve above 350 °C and becomes the major compound at 400 °C. The release of gaseous products was reported in reference 8. Laminate panels with aluminum foil bonded to both resin-rich surfaces developed surface bubbles beneath the foil during aging at 316 °C (ref. 8). This occurrence should be acknowledged when consideration is given to protecting composites with impervious coatings. The weight loss becomes linear with time between A and B and is attributed to normal thermal and oxidative reactions. After point B, the weight loss rate is accelerated by reason of the increase in surface area caused by the initiation and growth of surface microcracks that also allow easier penetration into the specimen by atmospheric oxygen. The cracking occurs at a much faster rate than observed with neat resin specimens and continually increases in depth with increasing aging time at equivalent temperatures. No asymptotic behavior is observed. The cracking can be attributed to the shrinkage of the polymer matrix during oxidation at the elevated temperature (refs. 9 to 11), increasing the mismatch in strain between the reinforcement and the matrix.

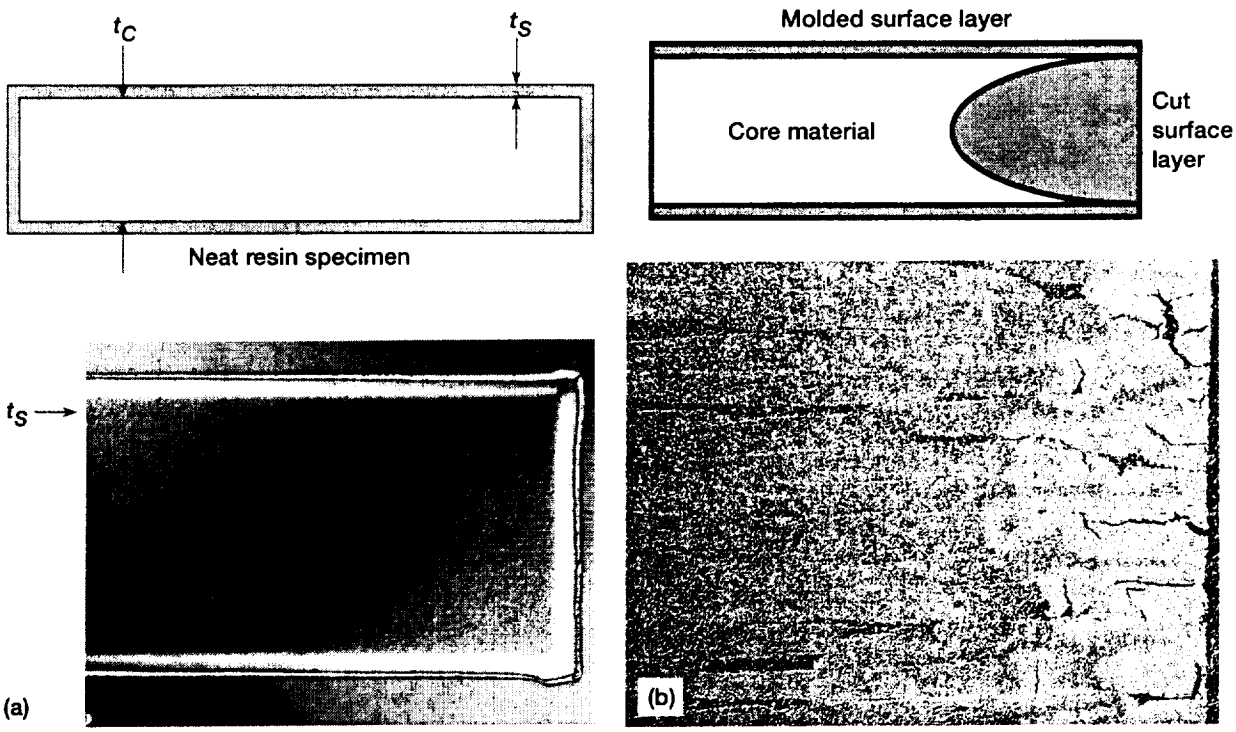

Figure 10.—Development of oxidized surface layer on neat resin and T650–35/PMR–15 composite after aging in air at elevated temperatures. (a) PMR–15 neat resin oxidized surface layer. Surface layer thickness, t_S; core thickness, t_C (ref. 7). (b) T650–35 composite oxidized surface layer.

Surface Layer Growth

Figure 10 shows a schematic of the development of an oxidized surface layer on both neat resin and fabric-reinforced composites. The layers in the neat resin (fig. 10(a), ref. 7) have a uniform and very small thickness throughout all outer surfaces. The thickness approaches a maximum of about 0.25 mm during aging at 204 °C. Surface layer growth data for neat resin specimens during aging at 204, 260, 288, and 316 °C are given in figure 11. All the data mass together below a 0.25-mm thickness. The data from specimens aged at 316 °C are in agreement with those published in references 6, 12, and 13. Even though reference 13 contains a number of misconceptions and misstatements, the data are reliable. There are differences in the initial portion of the curves, which is the time to approach the maximum thickness. Although the 204 °C aging data reach the maximum surface layer in about 750 hr, it takes longer for the other data to do so. The reason for the difference is based on the surface weight loss rates and the oxygen diffusion rates. The slopes of the curves of weight loss per unit surface area are 3.86×10^{-6}, 3.444×10^{-6}, 8.68×10^{-7}, and 2.09×10^{-7} gm/cm^2-hr for the 316, 260, and 204 °C data, respectively. Because the weight loss rate at 204 °C is much smaller than that at 316 °C, the surface of the specimen aged at the lower temperature loses less weight than the specimens aged at the higher temperatures and the outer surface moves inward at a slower rate than the interface. The oxygen is not significantly consumed in oxidative reactions until the maximum surface layer thickness has been established. The diffusion of the oxygen is hindered by the devouring of the reactant in the oxidative reactions at the higher temperatures. The data in figure 11 are in agreement with the coupled reaction-diffusion and chemical reaction models studied in reference 1.

In contrast, the surface layer for the composite (fig. 10(b)) is uniform for both resin-rich surfaces but has an elliptical shape at the cut surfaces. The greatest penetration is at the midplane of the specimen. The depth of penetration is dependent on the thickness of the specimen, with the deepest penetration occurring in the thickest material (ref. 10). This elliptical shape may be due to the increase in resin volume percent as one nears the center of the composite thickness. This has been observed and reported in reference 12. Nelson (ref. 13) examined the growth of edge cracks in PMR–15 and LARC–160 matrix composites. The thicknesses were kept constant and the crack progression into the composite was monitored with an x-ray-absorbing zinc iodide solution. A time-temperature superposition of the crack data was performed using an Arrhenius form for the shift factor. A direct correlation was found for a

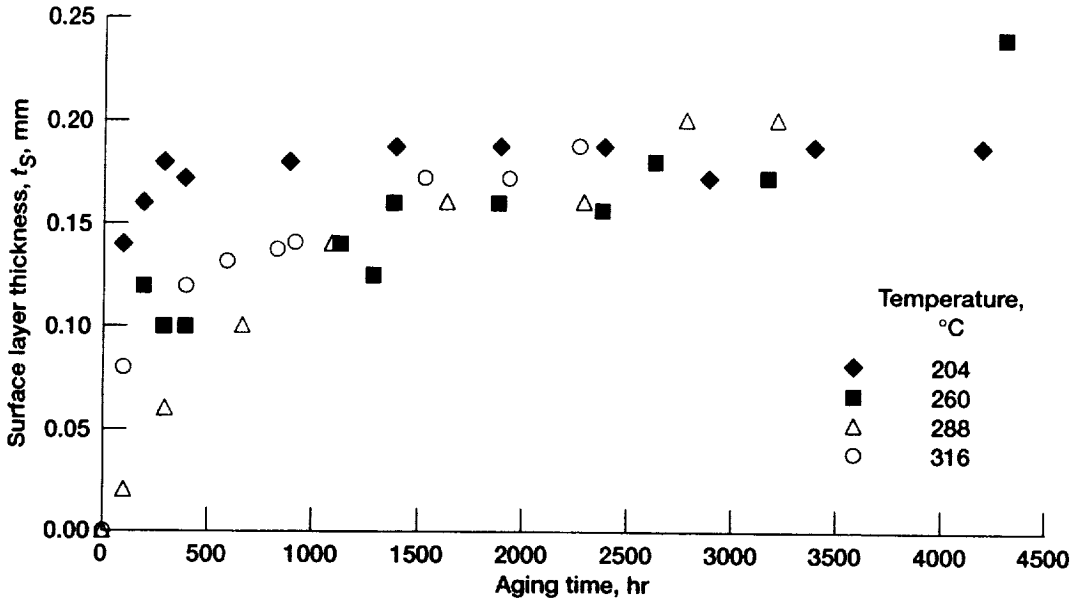

Figure 11.—Development of PMR–15 neat resin surface layer as function of aging time and temperature.

Celion/LARC–160 composite but not for a Celion/PMR–15 composite. The radiographic method that was used did not allow the parabolic-shaped edge damage (fig. 10(b)) to be detected and accounted for in the correlation.

Dimensional Changes

Figure 12 presents the data from the present study as a fraction of shrinkage in various dimensions of neat resin PMR–15 specimens. If the dimensional changes per unit length were constant throughout each dimension, the data would collapse onto one curve. They do not do so as evident from the plot of the 204 °C data, which show significant scatter in dimensional measurements from aging times of 1900 to 3300 hr. The reported measurement accuracy of the traveling microscope is ±0.00127 mm, well below the observed scatter. Fine surface cracks began to form around 2400 hr and they increased in number and crack width as time progressed. Surface cracks also were observed on specimens aged at 316 °C after 2800 hr. No severe dimensional changes were evident, perhaps because of the extreme differences in the magnitudes of the ordinate scales between the 204 and 316 °C data. No cracks were observed on the surfaces of specimens aged at 260 or 288 °C during their testing times. The data in figure 13 indicate that the polymer dimensional changes are related to the weight loss for specimens that were aged at 316 °C.

Figure 14 shows a plot of composite data of T650–35 fabric-reinforced PMR–15 aged at 316 °C with data from neat resin specimens. The data from the fabric-reinforced composites are not as would be expected in comparison with the neat resin data because the composites contain only a nominal 40 percent of resin. The composite data feature a rapid rise in through-the-thickness shrinkage during the first 250 hr of aging. This shrinkage is significantly more than the change in thickness exhibited by the neat resin specimens and is about equal to the rates of change for the neat resin lengths. The explanation is that there is a faster release of cure and postcure reaction products from the small composite specimens along the fiber-matrix interfaces. The specimens measured 75.2 by 3.3 by 2.5 mm nominally with the fibers oriented in the 75.2 direction. In contrast, all reaction products must be released from the neat resin specimens by diffusion.

Weight Loss Partitioning

It is assumed that the measured weight loss is due to the material lost in the formation of the surface layer, the loss of oxidized surface material, and the outward diffusion of the degradation products of the central bulk of the specimen, causing bulk volume shrinkage. The theoretical volume decrease can be obtained by dividing the

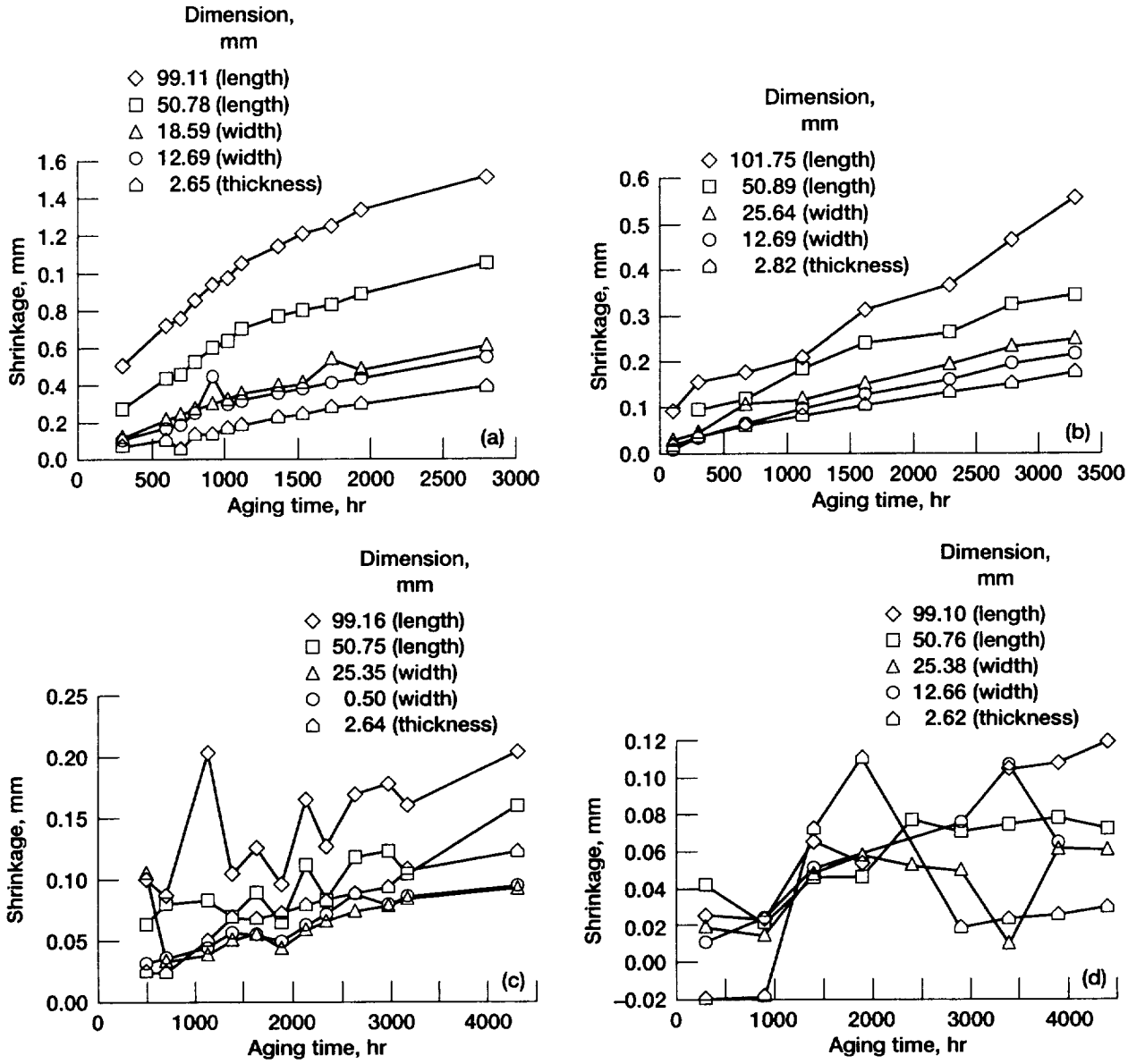

Figure 12.—Shrinkage of PMR–15 neat resin as function of aging time and dimensions. (a) Aging at 316 °C. (b) Aging at 260 °C. (c) Aging at 260 °C. (d) Aging at 204 °C.

measured weight loss by the polymer density. The measured volume loss can be calculated from the changes in specimen dimensions during aging. The difference between the measured volume loss and the calculated volume loss can be assumed to be due to shrinkage of the specimen that involves no weight loss if it is a positive difference. If it is a negative difference, some of the weight loss is coming from the core material and no thermal shrinkage of the core could be separated from the chemical degradation weight loss. Logically, some of the core shrinkage would be accompanied by a weight loss, so the calculated volume loss based on the total weight loss is not completely accurate. The value for the material density is in error. The volume loss would be greater than the actual amount. Although the distribution of the measured weight loss between surface loss and bulk polymer loss cannot be estimated by comparing the calculated volumes of the aged specimens with the calculated volumes of the initial unaged specimen dimensions, an indication of the central core shrinkage is apparent in the data presented in references 5 and 6. The shrinkage of PMR–15 neat resin specimens cured in nitrogen at 316 °C (fig. 15, ref. 6) appears to approach a maximum of about 0.6 percent after 801 hr of aging. Specimens aged in air at the same temperature and time show shrinkage values of 1 percent with no evidence of asymptotic behavior.

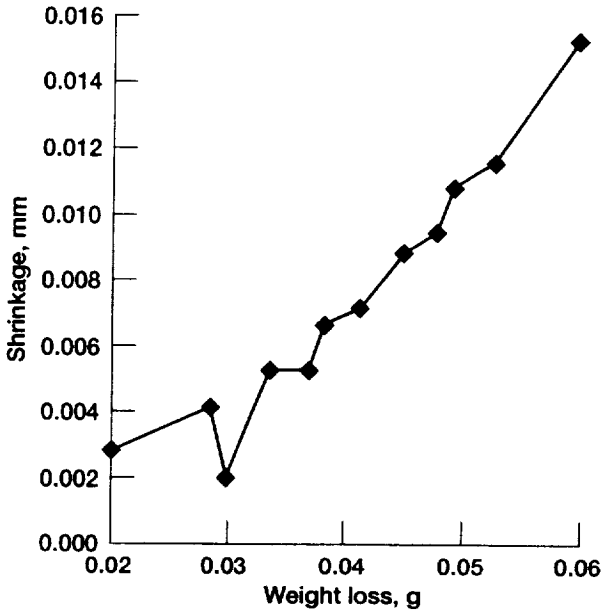

Figure 13.—Shrinkage of PMR–15 neat resin specimen length as function of specimen weight loss during aging at 316 °C.

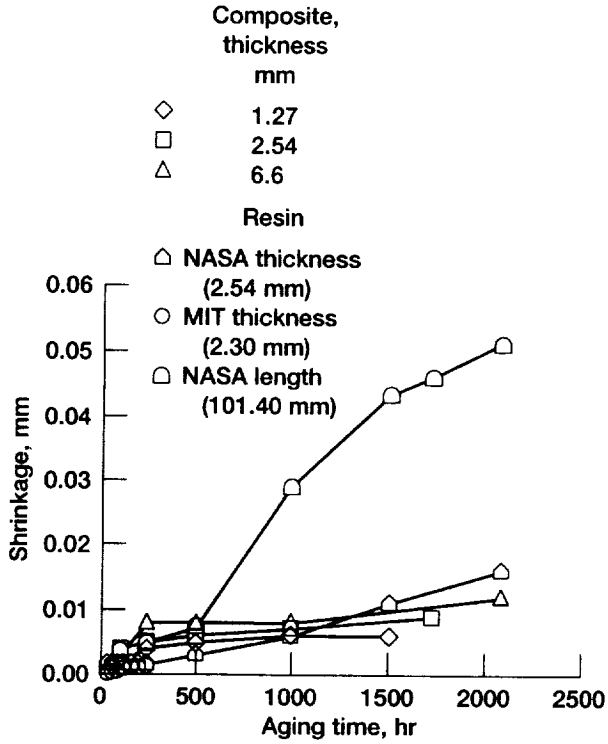

Figure 14.—Shrinkage of PMR–15 neat resin and composites during aging at 316 °C.

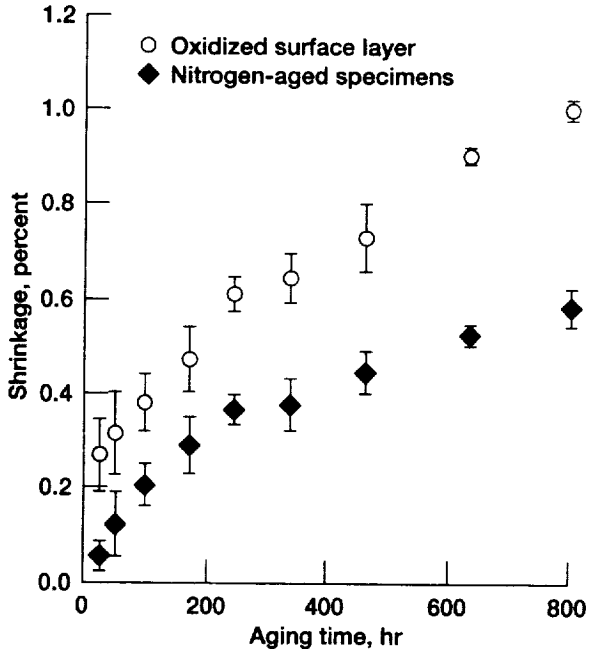

Figure 15.—Shrinkage of PMR–15 neat resin specimens aged in air and nitrogen at 316 °C as function of aging time (ref. 6).

TABLE V.—MEASURED WEIGHT LOSSES AND WEIGHT LOSSES CALCULATED FROM VOLUME CHANGES FOR PMR–15 AFTER AGING AT VARIOUS TEMPERATURES FOR DIFFERENT TIMES

Aging temperature, °C	Aging time, hr	Length, L, mm	Width, w, mm	Thickness, t, mm	Measured weight loss, ΔW, g	Calculated weight loss by volume difference, g	Difference in weight loss, g	Difference in volume, cm^3
316	2800	9.76	1.79	0.229	0.877	0.558	0.318	0.37
		9.75	1.21	.220	1.217	1.199	.017	.00
		4.97	1.21	.220	.472	.412	.059	.04
		4.97	1.21	.226	.450	.289	.161	.12
260	4000	9.89	2.53	0.258	0.274	0.349	−0.075	−0.05
		9.89	1.26	.260	.145	.011	.133	.10
		5.05	2.52	.252	.140	.186	−.046	−.03
		5.59	1.26	.248	1.926	−.034	1.961	1.48
204	4400	9.89	1.25	0.251	0.029	0.064	−0.035	−0.02
		9.90	2.53	.260	.046	.123	−.077	−.05
		5.06	2.52	.255	.027	.078	−.051	−.03
		5.06	1.26	.262	.016	.044	−.027	−.02
		5.07	1.25	.266	.017	.038	−.021	−.01

Table V presents values calculated from the measured weight loss differences and weight losses converted from volumes by multiplying by the composite density. At the lower two temperatures, these differences are consistently less than the weight losses calculated from the difference in volumes and weight losses of the starting material and the aged material. Calculations were made using the following formulas:

$$\frac{\Delta W}{\rho} - \Delta V = \Delta C \tag{1}$$

and

$$\Delta W - \Delta V\rho = \Delta D \tag{2}$$

where ΔW is the measured weight loss, ΔV is the measured loss in specimen volume, ρ is the measured specimen density, ΔC is the change in volume in the bulk of the specimen, and ΔD is the change in weight. The value of ΔC can be converted to a linear value by dividing by two times the specimen surface area to give the linear shrinkage in each dimension. The cut surfaces make up a small portion of the total surface area of a specimen, so the calculated values of shrinkage are reasonable. The mass loss ΔD is positive and decreases as the aging temperature decreases, whereas the shrinkage ΔC becomes negative in equation (2) because $\Delta V\rho$ becomes greater than ΔW. The data from this investigation seem to confirm the conclusions presented in reference 4; that is, there appear to be at least three mechanisms in operation during the thermal aging of PMR–15: a weight gain throughout the composite (not proven in this section), a temperature-dependent weight loss concentrated in the surface area of the composite and dominating the total degradation, and a smaller and less temperature-dependent weight decrease concentrated in the bulk of the composite.

If the weight loss were distributed between the surface oxidation and the core thermal degradation, it would seem logical to model it by a simple binomial equation of the form

$$\Delta W = Vx + Sy \tag{3}$$

where ΔW is the weight change over a specified period of time, V is the specimen volume, x is the specimen weight loss per unit volume, S is the specimen surface area, and y is the weight loss per unit surface area. The values for x and y could be determined by solving two simultaneous equations using values of V and S from two geometrically different specimens. The results of this analysis were not consistent, and therefore it is assumed that the weight loss mechanisms are more complex and the rates of weight loss are not constant throughout each of the two different sections of the specimens. This situation can only be described by more complex relationships.

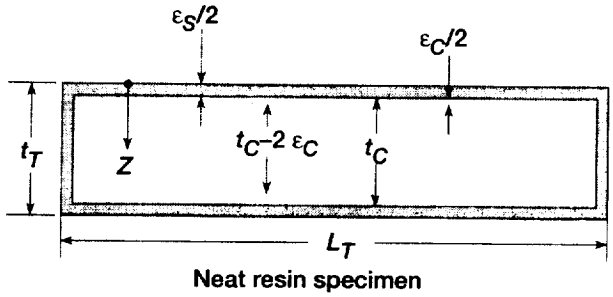

Figure 16.—Dimension notations for equations (4) to (6) describing shrinkage values. L_T, original length; t_C, core thickness; t_T, original thickness; ε_C, core shrinkage; ε_S, surface layer shrinkage; Z, distance from center of specimen.

One can easily derive relationships to calculate the amount of the surface weight loss and the total specimen volume shrinkage from dimensional change data measured during the aging of the neat resin specimens of PMR–15. Shrinkage due to the coefficient of thermal expansion (CTE) in cooling from the aging temperature to the room temperature will be ignored. The CTE calculations for PMR–15 aged at 316 °C are presented in reference 6. Treating the surface layer shrinkage and movement inward with the specimen surface as a strain called "pseudostrain," one can mathematically model the change in dimensions. For a neat resin specimen like the schematic in figure 16, the overall shrinkage at room temperature in each of the three dimensions can be calculated by using the following pseudostrain notations:

$$t_T\varepsilon_S + (t_i - 2t_S)\varepsilon_C = \Delta t \tag{4}$$

$$t_T\varepsilon_S + (w_i - 2t_S)\varepsilon_C = \Delta w \tag{5}$$

$$t_T\varepsilon_S + (L_i - 2t_S)\varepsilon_C = \Delta L \tag{6}$$

and

$$(t, w, \text{or } L) - 2t_s\varepsilon_S = \text{dimension of core material} \tag{7}$$

where

t_T original thickness of specimen, mm

ε_S surface layer shrinkage, mm/mm

t_S thickness of surface layer, mm

ε_C core shrinkage, mm/mm

w width of specimen, mm

L length of specimen, mm

Subscript:

i dimension at designated aging time

The thickness of the surface layer is the measured surface layer thickness after aging. The thickness approaches a constant value after a short period of time.

The values of the surface layer movement and the core material shrinkage can be calculated by simultaneously solving any two equations from maybe (4), (5), and (6). Three values of each were calculated solving three sets: (4) and (5), (4) and (6), and (5) and (6). For all three equations, $t_T\varepsilon_S$ is the same and cancels out in the calculations. Table VI presents the results of these calculations for neat resin specimens. As seen from the table, two significant results are evident: the first is that there is almost as much as 2 magnitudes of difference in the values of the two-dimensional decreases. The shrinkage of the surface is the larger. The surface layer thickness remained constant with varying specimen thickness so most of the shrinkage is due to the loss of surface material. The second is that the shrinkage of the surface shows large variations in calculated strains among the three combinations of equations. Because the surface recession measurements reflect surface layer shrinkage and surface movement inward, they do not agree with those calculated from bimetallic-type curvature measurements (ref. 6). When an aged specimen of PMR–15 was split through the center plane so that there were two bimetallic-type specimens, the resulting curvature was concave toward the core side. The strains calculated in reference 6 are measured along the length of the surface of the specimen and through the thickness. Also, the calculations used in reference 6 give values of the surface layer shrinkage in reference to the thermally induced shrinkage of the core material. Using as the core shrinkage (ref. 6) the polymer shrinkage values measured during aging in a nitrogen atmosphere, calculations utilizing these equation pairs show that the room temperature shrinkage strain of the surface layer is a compressive 1 percent strain after aging at 316 °C for 800 hr. The core shrinkage was 0.57 percent under the same time-temperature conditions. Experimentally proven in reference 14, this result suggests that any surface cracking that occurs from extended thermal cycling initiates at the elevated temperature and is intensified by the cyclic compressive forces experienced during cooldown cycles.

In the derivation of equations (4) to (7), it was tacitly assumed that the surface layer and the core material shrank homogeneously throughout each dimension. It is apparent that this is not true from examination of table VI. The three pairs of equations for each time and temperature combination give different values for the core shrinkage ε_C. The reason may be a variation in shrinkage strain in the core material with the change in the distance z in figure 16. Figure 17 shows a schematic of the physical state that the solution describes for each pair of equations (4) to (6) using the values of the three specimen dimensions. The calculated values of the strains only pertain to the volumes of material in the unshaded areas of the sketch. They show that there are differences as one scans across the specimen dimensions. The smallest dimension (2.4-mm thickness) is more sensitive to the surface layer shrinkage and surface material loss than the other two. In contrast, the changes in the specimen length dimension of 53.5 mm show that the changes are more representative of the central core material. The differences in the three calculated values of ε_C are consistent in that the magnitudes of the values from the equations are ranked in this order: equation (6) > equation (5) > equation (4). This suggests that shrinkage of the core decreases as one traverses through the thickness toward the center of the aged specimen (as z increases). Equations (4) and (5) represent material extending from the center to distances from the surface layer equivalent to the width and thickness, respectively. The calculated values of shrinkage for the pairs of equations containing the two smallest dimensions (~25 or ~12.5 and ~2.6 mm) consistently give the largest values of the three calculations. This indicates that the cores having the lesser thickness experience greater overall shrinkage than the thicker specimens. As one traverses from the thickness centerline toward the thickness or width surfaces, the amount of shrinkage experienced by the polymer increases. The values of the three ε_C calculations at the same temperatures and the calculated through-the-thickness strains are also shown in table V. The values from equation (4) are subtracted from the values from equation (3) and are compared with the values from equation (6). The results should equal the shrinkage calculated with the strain from equation (6). The agreement is very good and verifies the suitability of the analysis for modeling the degradation process.

Compression Property Changes

Thick composite specimens aged at 260 °C for 20 000 hr were sliced into 2.54-mm-thick slabs parallel to the resin-rich surfaces as shown in table IV (refs. 15 and 16). The room temperature compression properties were measured and are also included in this figure. It is apparent that the surface layer is damaged more severely than the material in the specimen core. It is also significant that there is little difference in the strengths of the two central specimens and that the modulus remains constant throughout the cross section, probably because the moduli were measured at the lower end of the stress-strain curve (between 500 and 15 000 microstrain, ref. 15) and the graphite-

TABLE VI.—CORE AND SURFACE SHRINKAGE AND STRAIN FOR PMR–15 NEAT RESIN SPECIMENS AGED AT VARIOUS TEMPERATURES FOR 2800[a] AND 4400 HOURS

Aging conditions		Equation pairs[b]	Length, L, mm	Width, w, mm	Thickness, t, mm	Shrinkage, mm		Strain	
Temperature, °C	Time, hr					Core	Surface	Surface	Core
204	4400	(4) and (5)	99.093	25.3677	2.64	0.044	0.016	0.001	0.001
			99.068	12.6034	2.532	.0663	.0425	.003	.003
			50.734	25.593	2.586	.2704	−.2183	−.009	−.009
			50.7746	12.626	2.704	.0108	.0611	.005	.005
			50.787	12.7356	2.65	.0372	.0548	.004	.004
		(5) and (6)	99.093	25.3677	2.64	−0.0157	0.0757	0.029	0.033
			99.068	12.6034	2.532	−.3893	.4981	.197	.231
			50.734	25.593	2.586	.2704	−.2183	−.084	−.099
			50.7746	12.626	2.704	.0108	.0611	.023	.026
			50.787	12.7356	2.65	.0372	.0548	.021	.024
		(4) and (6)	99.093	25.3677	2.64	0.0283	0.0317	0.012	0.014
			99.068	12.6034	2.532	−.323	.4318	.171	.200
			50.734	25.593	2.586	.018	.0341	.013	.015
			50.7746	12.626	2.704	.0381	.0338	.013	.015
			50.787	12.7356	2.65	.0634	.0286	.011	.013
260	4300	(4) and (5)	99.1743	25.5473	2.675	0.1473	0.061	0.002	0.002
			99.1565	12.733	2.586	.0172	.1885	.015	.015
			50.7085	25.342	2.617	.0325	.0817	.003	.003
			50.7695	12.7249	2.682	−.1059	−4.7796	−.376	−.389
		(5) and (6)	99.1743	25.5473	2.675	0.1473	0.061	0.023	0.027
			99.1565	12.733	2.586	.0172	.1885	.073	.088
			50.7085	25.342	2.617	.0325	.0817	.031	.038
			50.7695	12.7249	2.682	−.1059	−4.7796	−1.782	−2.13
			50.734	12.681	2.551	.2197	.7595	.298	.356
		(4) and (6)	99.1743	25.5473	2.675	0.1169	0.0914	0.034	0.041
			99.1565	12.733	2.586	.1274	.0783	.030	.036
			50.7085	25.342	2.617	.0259	.0883	.034	.041
			50.7695	12.7249	2.682	−5.0785	.193	.072	.086
288	4000	(4) and (5)	101.7544	25.3634	2.776	0.2866	0.2696	0.097	0.011
			101.7621	12.6837	2.806	.3399	.2240	.080	.018
			50.7459	25.9245	2.835	.1035	.2252	.079	.009
			51.1632	12.7305	2.844	.3822	−.0284	.010	.002
			50.7766	12.6987	2.843	−.1113	.2009	.071	.016
		(5) and (6)	101.7544	25.3634	2.776	0.0881	0.4681	0.169	0.019
			101.7621	12.6837	2.806	.0434	.5205	.185	.042
			50.7459	25.9245	2.835	.0421	.2866	.101	.011
			51.1632	12.7305	2.844	−.2119	.5657	.199	.046
			50.7766	12.6987	2.843	.0247	.0649	.023	.005
		(4) and (6)	101.7544	25.3634	2.776	0.3743	0.1819	0.066	0.007
			101.7621	12.6837	2.806	.3831	.1808	.064	.015
			50.7459	25.9245	2.835	.1452	.1835	.065	.007
			51.1632	12.7305	2.844	.1777	.1761	.062	.014
			50.7766	12.6987	2.843	−.0864	.1760	.062	.014
316	2800	(4) and (5)	99.1159	18.6139	2.697	0.2136	1.2978	0.070	0.071
			99.1108	12.6759	2.604	.1733	1.3418	.106	.109
			50.7848	12.7533	2.642	.1572	.919	.072	.075
			50.734	12.681	2.668	.102	.8772	.069	.072
		(5) and (6)	99.1159	18.6139	2.697	1.1094	0.402	0.149	0.177
			99.1108	12.6759	2.604	1.3762	.4036	.155	.185
			50.7848	12.7533	2.642	.6444	.4318	.163	.194
			50.734	12.681	2.668	.5716	.4076	.153	.181
		(4) and (6)	99.1159	18.6139	2.697	1.0880	0.4234	0.157	0.186
			99.1108	12.6759	2.604	1.1080	.4071	.156	.186
			50.7848	12.7533	2.642	.6359	.4403	.167	.198
			50.734	12.681	2.668	.5649	.4143	.155	.184

[a]Aged at 316 °C.

[b]Pseudostrain equations (4), (5), and (6) used to simultaneously calculate values of surface layer movement and core material shrinkage. See discussion in section on Weight Loss Partitioning, p. 14.

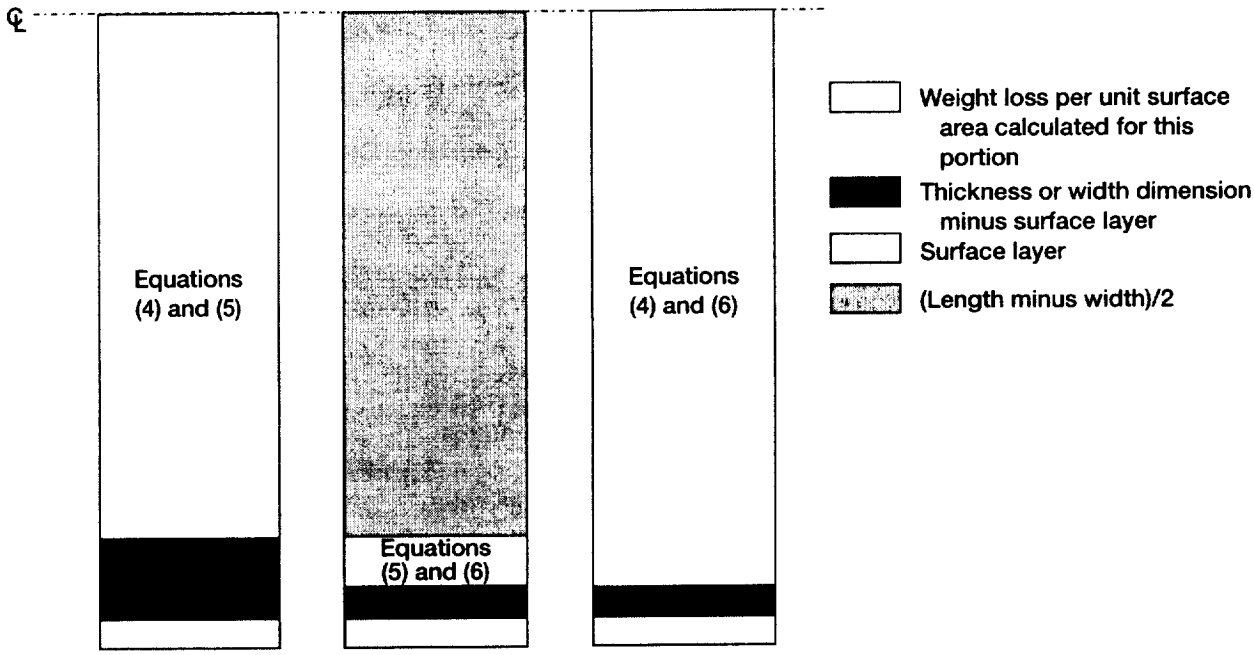

Figure 17.—Specimen areas described by equations (4) to (6).

fiber-reinforcement modulus does not change unless the fibers begin to oxidize. The strength and modulus of the unaged material were about 700 MN/m^2 and 100 GN/m^2, respectively. The damaged surface layer retained 20 percent of the original strength and 57 percent of the unaged modulus. One other critical point to note is that the visibly undamaged central core has still lost a significant amount of its compression strength. Similar invisible damage has been observed and reported for polyimide and epoxy matrix composites that have been aged for up to 50 000 hr at 177 and 288 °C (ref. 17). It was stated in reference 15 that specimens made with four and eight plies of T650–35/PMR–15 were aged long enough for the entire thickness of each specimen to contain damaged surface layer material. These totally damaged specimens retained 20 percent of the original strength and the eight-ply specimen retained 60 percent of the unaged modulus. Retained moduli of the four-ply specimens were variable.

SUMMARY

Physical and chemical changes occur as a function of time and location in PMR–15 neat resin and composites during aging in air at elevated temperatures. These changes initiate at the outer surfaces of both materials and progress inward following the oxygen as it proceeds by diffusion into the central core of each material. Microstructural changes cause changes in density, material shrinkage (strains), glass transition temperature, dimension, dynamic shear modulus, and compression properties. These changes also occur slowly, dividing the polymer material into two distinct parts: a visibly undamaged core section between two visibly damaged surface layers. The surface layer has a significant effect on the compression properties of thinner specimens, but the visibly undamaged core material controls these properties for specimens having eight or more plies. The minimum compression strength appears to be around 20 percent of the normalized strength because the strength is a property dominated by the matrix properties. In contrast, the modulus is a fiber-dependent property and does not appear to approach a limiting value as does the strength.

The study demonstrated that three mechanisms are involved in the degradation of PMR–15 during aging at elevated temperatures: a weight gain, a small weight fraction bulk material weight loss, and a large mass fraction weight loss concentrated at the surface of the polymer or composite. At the higher temperatures (260 °C and above), the surface loss predominates. Below 260 °C, the surface loss and the bulk core loss become more equivalent. Between 175 and 260 °C, the initial weight change is due to a weight gain mechanism with a visible lifetime that diminishes as the aging temperature increases.

REFERENCES

1. Cunningham, Ronan A.: High Temperature Degradation Mechanisms in Polymer Matrix Composites. NASA CR–206189, 1997.
2. Patekar, Kaustubh A.: Long Term Degradation of Resin for High Temperature Composites. S.M. Thesis, Massachusetts Institute of Technology, 1998.
3. Parvatareddy, H., et al.: Environmental Aging of High-Performance Polymeric Composites Effects on Durability. Comp. Sci. Tech., vol. 53, no. 4, 1995, pp. 399–409.
4. McManus, H.L.; and Cunningham, R.A.: Materials and Mechanics Analyses of Durability Tests for High-Temperature Polymer Matrix. High Temperature and Environmental Effects on Polymeric Composites, 2nd vol., ASTM Special Technical Publication 1302, 1997, pp. 1–17.
5. Cunningham, Ronan A.: Coupled Diffusion-Reaction Models for Predicting the Distribution of Degradation in Polymer Matrix Composites. Proceedings of the ASME Aerospace Division International Mechanical Engineering Congress and Exposition, ASME, New York, NY, 1996, pp. 353–359.
6. Tsuji, Luis C.; McManus, Hugh L.; and Bowles, Kenneth J.: Mechanical Properties of Degraded PMR–15 Resin. Time Dependent and Nonlinear Effects in Polymers and Composites, ASTM Special Technical Publication 1357, 2000, pp. 3–17.
7. Bowles, Kenneth J.; McCorkle, Linda; and Ingrahm, Linda: Comparison of Graphite Fabric Reinforced PMR–15 and Avimid N Composites After Long-Term Isothermal Aging at Various Temperatures. J. Adv. Mat. (NASA/TM—1998-107529), vol. 30, no. 1, 1998, pp. 27–35.
8. Hurwitz, F.I.; and Whittenberger, J.D.: The Effect of a Coating on the Thermo-Oxidative Stability of Celion 6000 Graphite Fiber/PMR–15 Polyimide Composites. Comp. Tech. Rev., vol. 5, 1983, pp. 109–114.
9. Madhukar, Madhu S.; Kosuri, Ranga P.; and Bowles, Kenneth J.: Monitoring Fiber Stress During Curing of Single Fiber Glass- and Graphite-Epoxy Composites. NASA TM–4568, 1995.
10. Penn, L.S., et al.: The Effect of Matrix Shrinkage on Damage Accumulation in Composites. J. Compos. Mater., vol. 23, 1989, pp. 570–586.
11. Simpson, M.; Jacobs, P.M.; and Jones, F.R.: Generation of Thermal Strains in Carbon Fiber-Reinforced Bismalaemide (PMR–15) Composites. 3.—A Simultaneous Thermogravimetric Mass-Spectral Study of Residual Volatiles and Thermal Microcracking. CPSOA, vol. 22, no. 2, 1991, pp. 105–112.
12. Campbell, F.C.; Mallow, A.R.; and Browning, C.E.: Porosity in Carbon-Fiber Composites—An Overview of Causes. J. Adv. Mat., vol. 26, no. 4, 1995, pp. 18–33.
13. Nelson, J.B.: Edge Crack Growth of Thermally Aged Graphite/Polyimide Composites. NASA TM–85763, 1984.
14. Bowles, Kenneth J.; and Nowak, Gregory: Thermo-Oxidative Stability Studies of Celion 6000/PMR–15 Unidirectional Composites, PMR–15, and Celion 6000 Fiber. J. Compos. Mater., vol. 22, 1988, pp. 966–985.
15. Bowles, Kenneth J.: Thermal and Mechanical Durability of Graphite-Fiber-Reinforced PMR–15 Composites; Revised. Proceedings of the Third International Conference on Progress in Durability Analysis of Composite Systems (NASA/TM—1998-113116), K.L. Reifsnider, David A. Dillard, and Albert H. Cardon, eds., Balkema, Rotterdam, 1997.
16. Bowles, K.J.; Roberts, G.D.; and Kamvouris, J.E.: Long-Term Isothermal Aging Effects on Carbon Fabric-Reinforced PMR–15 Composites: Compression Strength. High Temperature and Environmental Effects on Polymeric Composites, ASTM Special Technical Publication 1302, 1997, pp. 175–190.
17. Kerr, J.R.; and Haskins, J.F.: Effects of 50,000 h of Thermal Aging on Graphite/Epoxy and Graphite/Polyimide Composites. AIAA J., vol. 22, 1984, pp. 96–102.

REPORT DOCUMENTATION PAGE

Form Approved
OMB No. 0704-0188

1. AGENCY USE ONLY (*Leave blank*)	2. REPORT DATE	3. REPORT TYPE AND DATES COVERED
	July 2001	Technical Memorandum

4. TITLE AND SUBTITLE

Longtime Durability of PMR–15 Matrix Polymer at 204, 260, 288, and 316 °C

5. FUNDING NUMBERS

WU–708–31–13–00

6. AUTHOR(S)

Kenneth J. Bowles, Demetrios S. Papadopoulos, Linda L. Inghram, Linda S. McCorkle, and Ojars V. Klan

7. PERFORMING ORGANIZATION NAME(S) AND ADDRESS(ES)

National Aeronautics and Space Administration
John H. Glenn Research Center at Lewis Field
Cleveland, Ohio 44135–3191

8. PERFORMING ORGANIZATION REPORT NUMBER

E–12545

9. SPONSORING/MONITORING AGENCY NAME(S) AND ADDRESS(ES)

National Aeronautics and Space Administration
Washington, DC 20546–0001

10. SPONSORING/MONITORING AGENCY REPORT NUMBER

NASA TM—2001-210602

11. SUPPLEMENTARY NOTES

Kenneth J. Bowles and Ojars V. Klan, NASA Glenn Research Center; Demetrios S. Papadopoulos, University of Akron, 302 Buchtel Mall, Akron, Ohio 44325–0001; Linda L. Inghram and Linda S. McCorkle, Ohio Aerospace Institute, 22800 Cedar Point Road, Brook Park, Ohio 44142. Responsible person, Demetrios S. Papadopoulos, UNAK, 216–433–6662.

12a. DISTRIBUTION/AVAILABILITY STATEMENT

Unclassified - Unlimited
Subject Category: 24 Distribution: Nonstandard

Available electronically at http://gltrs.grc.nasa.gov/GLTRS

This publication is available from the NASA Center for AeroSpace Information, 301–621–0390.

12b. DISTRIBUTION CODE

13. ABSTRACT ***(Maximum 200 words)***

Isothermal weight loss studies at the Glenn (Lewis) Research Center were conducted at four temperatures (204, 260, 288, and 316 °C) with specimens of varied geometric shapes to investigate the mechanisms involved in the thermal degradation of PMR–15. Both neat resin behavior and composite behaviors were studied. Two points of interest in these studies are the role(s) of oxygen in the mechanisms involved in the thermo-oxidative degradation of these composite materials and the dimensional changes that occur during their useable lifetime. Specimen dimensional changes and surface layer growth were measured and recorded. It was shown that physical and chemical changes take place as a function of time and location in PMR–15 neat resin and composites as aging takes place in air at elevated temperatures. These changes initiate at the outer surfaces of both materials and progress inward following the oxygen as it proceeds by diffusion into the central core of each material. Microstructural changes cause changes in density, material shrinkage (strains), glass transition temperature, dimension, dynamic shear modulus, and compression properties. These changes also occur slowly dividing the polymer material into two distinct parts: a visibly undamaged core section between two visibly damaged surface layers. The surface layer has a significant effect on compression properties of thinner specimens, but the visibly undamaged core material controls these properties for specimens having eight or more plies. It was demonstrated that there are three different mechanisms involved in the degradation of PMR–15 during aging at elevated temperatures. These are a weight gain, a small weight fraction bulk material weight loss, and a large mass fraction weight loss concentrated at the surface of the polymer or composite. At the higher temperatures (260 °C and above), the surface loss predominates. Below 260 °C, the surface loss and the bulk core loss become more equivalent. Between 175 and 260 °C, the initial weight change is due to a weight gain mechanism with a visible lifetime that diminishes as the aging temperature increases.

14. SUBJECT TERMS

Matrix polymers; Mechanisms oxidation degradation; Thermal damage; Polymer shrinkage composites; Physical properties; Physical changes; Mechanical properties

15. NUMBER OF PAGES

24

16. PRICE CODE

17. SECURITY CLASSIFICATION OF REPORT	18. SECURITY CLASSIFICATION OF THIS PAGE	19. SECURITY CLASSIFICATION OF ABSTRACT	20. LIMITATION OF ABSTRACT
Unclassified	Unclassified	Unclassified	